Bound states and scattering in quantum waveguides coupled laterally through a boundary window

P. Exner,[a,b] P. Šeba,[a,b] M. Tater,[a] and D. Vaněk[c]

a) Nuclear Physics Institute, Academy of Sciences
CZ–25068 Řež near Prague
b) Doppler Institute, Czech Technical University,
Břehová 7, CZ–11519 Prague,
c) Departmant of Mathematics, FNSPE, CTU,
Trojanova 13, CZ–12000 Prague, Czech Republic

We consider a pair of parallel straight quantum waveguides coupled laterally through a window of a width ℓ in the common boundary. We show that such a system has at least one bound state for any $\ell > 0$. We find the corresponding eigenvalues and eigenfunctions numerically using the mode–matching method, and discuss their behavior in several situations. We also discuss the scattering problem in this setup, in particular, the turbulent behavior of the probability flow associated with resonances. The level and phase–shift spacing statistics shows that in distinction to closed pseudo–integrable billiards, the present system is essentially non–chaotic. Finally, we illustrate time evolution of wave packets in the present model.

I Introduction

Spectral and scattering properties of quantum particles whose motion is confined to nontrivial subsets of $\mathbb{R}^n$ represented until recently rather textbook examples or technical tools used in proofs. There are several reasons why these problems attracted a wave of interest in last few years . The most mathematical among them stems from the observation that, roughly speaking, one can choose the region in such a way that the spectrum of the corresponding Neumann Laplacian coincides with a chosen set[1,2]; of course, the boundary of such a region may be in general rather complicated.

On the other hand, even regions with nice boundaries may exhibit various unexpected properties manifested, for instance, in spectra of the corresponding Dirichlet Laplacians. A prominent example is the existence of bound states, *i.e.*, localized solutions to the free Schrödinger equation, in infinitely stretched regions such as bent, branched or crossed tubes of a constant cross section — see, *e.g.*, Refs. 3–7; more references are given in the review paper[8].

I.1 Quantum wire systems

A strong motivation to study such bound states and related resonance effects[9–11] comes from recent developments in semiconductor physics, because they can be used as models of electron motion in so–called *quantum wires, i.e.*, tiny strips of a very pure semiconductor material, and similar structures. Let us briefly recall key features of such systems; more details and a guide to physical literature can be found in Ref. 8.

Characteristic properties of the semiconductor microstructures under consideration are *small size,* typically from tens to hundreds of nm, *high purity,* which means that the electron mean free path can be a few μm or even larger, and *crystallic structure.* In addition, boundaries of the microstrucures consist usually of an interface between two different semiconductor materials; the electron wavefuction are known to be suppressed there.

Behavior of an electron in such a "mesoscopic" system structure is, of course, governed by the many–body Schrödinger equation describing its interaction with the lattice atoms including the boundary, external fields, and possible impurities. The mentioned properties allow us, however, to adopt several simplifying assumptions. As we have said the mean free path is typically two or three orders of magnitude greater than the size of the structure; hence the electron motion can be assumed in a reasonable approximation as *ballistic, i.e.*, undisturbed by impurity scattering.

The most important simplification comes from the crystallic structure. The one–electron Hamiltonian as a Schrödinger operator with a periodic potential exhibits an absolutely continuous spectrum — see Ref. 12, Sec.XIII.16 — in the solid–state physics language one says that the electron moves in the lattice as *free* with some effective mass m^*. The latter changes, of course, along the spectrum but one can regard it as a constant when we restrict our attention to the physically interesting part of the valence band; recall that its value may differ substantially from the true electron mass, for instance, one has $m^* = 0.067\, m_e$ for GaAs which is the most common semiconductor material used in mesoscopic devices.

This property together with the wavefunction suppression at the interfaces makes natural to model electrons in a quantum wire system as free (spinless) particles living in the corresponding spatial region with the *Dirichlet condition* on its boundary; an interaction term must be added only if the whole structure is placed into an external field. This is the framework in which the mentioned curvature–induced bound states and resonances were studied. However, the physical conclusions one can draw from it are not restricted to mesoscopic devices: the results are useful for description of other "new" quantum systems[13] and provide fresh insights into the classical theory of electromagnetic waveguides[14–16].

I.2 Motivation of the present work

Apart from these practical reasons, the curvature–induced bound states provide at the same time a warning example showing that an intuition based on semiclassical concepts may fail when dealing with quantum systems. It is well known, for instance, that low–dimensional Schrödinger operators have bound states for an arbitrarily small coupling constant as long as the potential is not repulsive in the mean and decays sufficiently fast at infinity[17,18]. A common wisdom, however, is that this is rather an exception, and that the number of bound states of a quantum system is at least *roughly* proportional to the classically allowed volume of the phase–space. The waveguide systems in question illustrate that this is not true, because they can exhibit in principle *any* number of bound states, while having *no* closed classical trajectories with the exception of an obvious zero–measure set.

In this paper we are going to consider another example of that kind, this time consisting of two straight parallel quantum waveguides. We suppose that they have a common boundary which has a window of a width ℓ allowing the particle to leak from one duct to the other. This an idealized setup for several recently studied quantum–wire systems — see Refs. 19–22. Using a variational argument we shall show that such a system has always at least one bound state, *i.e.*, an isolated eigenvalue below the threshold of the continuous spectrum. Moreover, the system can have any prescribed number of bound states provided the window width is chosen large enough. These conclusions follow from simple estimates; however, they tell us nothing about the corresponding wavefunctions and more detailed dependence of the bound–state energies on the parameters. To this aim, we shall formulate in Section 4 a method to solve the problem numerically using the mode–matching technique. In particular, we shall discuss how the first eigenvalue emerges from the continuum as the window opens.

Interesting properties of the system are not exhausted by this. The coupling between the wavefunctions in the "arms" and the connecting region allows the particle to tunnel betwen different transverse modes, so the scattering matrix is nontrivial; one naturally expects it to have resonances with properties similar to those of the bound states below the first transverse–mode energy. It is not easy to prove the existence of such resonances, because there is no natural parameter in the problem which would make it possible to tune the intermode coupling. Neither the window width ℓ, nor replacing the "empty" window by an "opaque" one with a suitable point interaction as in Ref. 23 allow for a sensible perturbation theory, because in both cases the unperturbed bound state disappears as the coupling is switched out. Hence we rely again on a numerical analysis based on the mode–matching technique; the results confirm our expectation about the resonance character of the scattering and its dependence on parameters of the problem.

There is one more interesting aspect. The corresponding classical system of coupled ducts is pseudo–integrable, its phase space being of genus three. Other systems of that type have been recently studied[24,25]; it was shown that their quantum couterparts exhibit a chaotic behaviour. One asks naturally whether a similar effect

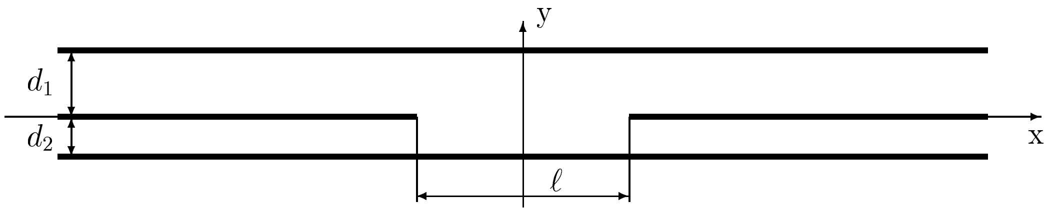

Figure 1: Laterally coupled quantum waveguides

can be observed here. To find the level–spacing distribution of the bound states, a very wide window is needed to produce a large number of eigenvalues. At the same time, the spectrum has to be unfolded, *i.e.*, rescaled so that the mean spacing does not change along it. The result suggests spacing distribution is then sharply localized around a fixed value, hence there is no chaos. This is not surprising, since all the bound–state wavefunctions have transversally the shape of the first mode, co effectively they correspond to a one–dimensional system. What is less trivial is that the spacing distribution of the scattering phase shifts also does not witness of a fully developed chaos; this suggests that repeated reflections are an essential ingredient of the chaotic behavior of particles in bounded pseudo–integrable billiards.

The above mentioned scattering analysis relies on the stationary approach. The time evolution of wave packets would deserve a separate study. In this paper we limit ourselves to a single example: in the concluding section we present a numerical method to solve the corresponding time–dependent Schrödinger equation, which allows us to draw some qualitative conclusions about time delay in the scattering on the connecting window.

II Preliminaries

The system we are going to study is sketched on Fig. 1. We consider a Schrödinger particle whose motion is confined to a pair of parallel strips of widths d_1, d_2, respectively. For definiteness we assume that they are placed to both sides of the x–axis, and they are separated by the Dirichlet boundary everywhere except in the interval $(-a, a)$; we shall denote this configuration space by Ω and $\ell := 2a$. Putting $\hbar^2/2m = 1$, we may identify the particle Hamiltonian with the Dirichlet Laplacian,

$$H \equiv H(d_1, d_2; \ell) := -\Delta_D^\Omega , \tag{2.1}$$

on $L^2(\Omega)$ defined in the standard way — see Ref. 12, Sec.XIII.15 — since the boundary of Ω has the segment property, it acts as the usual Laplace operator with the Dirichlet condition at the boundary.

A simple bracketing argument[12] shows that H has bound states for all ℓ large enough. Let us first introduce some notation. Set $d := \max\{d_1, d_2\}$ and $D :=$

$d_1 + d_2$, and furthermore

$$\nu := \frac{\min\{d_1, d_2\}}{\max\{d_1, d_2\}}\,.$$

We shall also use $\mu_d := \left(\frac{\pi}{d}\right)^2$, and μ_D, μ_ℓ corresponding in the same way to D and ℓ , respectively. Cutting now Ω by the additional Neumann or Dirichlet boundaries parallel to the y–axis at $x = \pm a$, we get $H_t^{(N)} \oplus H_c^{(N)} \le H \le H_t^{(D)} \oplus H_c^{(D)}$, where the "tail" part corresponds to the four halfstrips and the rest to the central part with the Neumann and Dirichlet condition on the vertical boundaries, respectively.

Since $\sigma_{ess}(H_t^{(j)}) = [\mu_d, \infty)$, $j = N, D$, the same is by the minimax principle true for H , and possible isolated eigenvalues of H are squeezed between those of $H_c^{(j)}$, $j = N, D$. The Neumann estimate tells us that

$$\inf \sigma(H(d_1, d_2; \ell)) \,\ge\, \mu_D \,=\, \mu_d(1+\nu)^{-2}\,. \tag{2.2}$$

On the other hand, H has an eigenvalue below μ_D provided $H_c^{(D)}$ does, which is true if $\mu_D + \mu_\ell \le \mu_d$; this shows that a sufficient condition for $H(d_1, d_2; \ell)$ to have at least a bound state is that the length of the opening satisfies the inequality

$$\ell \,\ge\, \frac{d(1+\nu)}{\sqrt{\nu(\nu+2)}}\,. \tag{2.3}$$

If $\nu = 1$, the coefficient on the right side is $2/\sqrt{3} \approx 1.155$; it grows as Ω becomes more asymmetric.

More generally, the number of eigenvalues of $H_c^{(D)}$ is $N_D := \left[\sqrt{(\mu_d - \mu_D)/\mu_\ell}\right]$, where $[\cdot]$ denotes the entire part (recall that since $D \le 2d$, the first transversally excited state is already above μ_d), while the number of the "Neumann" eigenvalues is $N_N := 1 + N_D$; this means that the number of bound states of $H(d_1, d_2; \ell)$ satisfies the inequality

$$\left[\frac{\ell}{d}\,\frac{\sqrt{\nu(\nu+2)}}{1+\nu}\right] \,\le\, N \,\le\, 1 \,+\, \left[\frac{\ell}{d}\,\frac{\sqrt{\nu(\nu+2)}}{1+\nu}\right]\,. \tag{2.4}$$

We see that $H(d_1, d_2; \ell)$ has isolated eigenvalues, at least for ℓ large enough, despite the absence of (a nonzero–measure set of) closed classical trajectories mentioned in the introduction. In heuristic terms, this may be understood as a manifestation of the fact that the semi-infinite "spikes" of the opened barrier between the two ducts are capable of reflecting a *quantum* particle due to a finite smearing of the wavepacket. In the same way, one finds that the mth eigenvalue μ_m of $H(d_1, d_2; \ell)$ is estimated by

$$\left(\frac{m-1}{\lambda}\right)^2 \,\le\, \frac{\mu_m}{\mu_d} \,-\, \frac{1}{(1+\nu)^2} \,\le\, \left(\frac{m}{\lambda}\right)^2, \tag{2.5}$$

where $\lambda := \ell/d$, and that the critical value $\lambda_m \equiv \ell_m/d$ at which mth eigenvalue appears satisfies the bounds

$$\frac{(m-1)(1+\nu)}{\sqrt{\nu(\nu+2)}} \,\le\, \lambda_m \,\le\, \frac{m(1+\nu)}{\sqrt{\nu(\nu+2)}}\,. \tag{2.6}$$

To learn more about the dependence of the eigenvalues and the corresponding eigenfunctions on λ and ν, we have to use a different technique.

III Existence of bound states

The above existence argument giving (2.3) is a crude one; in fact, there is no lower bound on the window width as the following result shows:

Theorem: $H(d_1, d_2; \ell)$ has an isolated eigenvalue in $[\mu_D, \mu_d)$ for any $\ell > 0$.

Proof: We modify for the present purpose the variational argument of Ref. 6; see also Ref. 8, Sec.2. Without loss of generality we may assume that $d_2 \le d_1 = d$. The transverse ground–state wavefunction is then

$$\chi_1(y) := \begin{cases} \sqrt{\frac{2}{d_1}}\,\sin(\kappa_1 y) & \dots \quad y \in (0, d_1) \\ 0 & \dots \quad \text{otherwise} \end{cases}$$

where $\kappa_1 := \sqrt{\mu_d}$; similarly we define the transverse ground state in the opening,

$$\eta_1(y) := \sqrt{\frac{2}{D}}\,\sin(K_1(d_1 - y))$$

with $K_1 := \sqrt{\mu_D}$. For any $\Phi \in D(H)$ we put

$$q[\Phi] := \|H\Phi\|^2 - \mu_d \|\Phi\|^2$$

(if not marked explicitly, the norms always refer to $L^2(\Omega)$).

Since the essential spectrum of H starts at μ_d, we have to find a trial function Φ such that $q[\Phi] < 0$; it has to belong to the form domain $Q(H)$ which means, in particular, that it must be continuous inside Ω but not necessarily smooth. Notice first that if $\Phi(x, y) = \varphi(x)\chi_1(y)$, we have

$$q[\Phi] = \|\varphi'\|^2_{L^2(I\!R)}\,. \tag{3.1}$$

To make the longitudinal contribution to the kinetic energy small, we use an external scaling. We choose an interval $J := [-b, b]$ for a positive $b > a$ and a function $\varphi \in \mathcal{S}(I\!R)$ such that $\varphi(x) = 1$ if $x \in J$; then we define the family $\{\varphi_\sigma :\, \sigma > 0\}$ by

$$\varphi_\sigma(x) := \begin{cases} \varphi(x) & \dots \quad |x| \le b \\ \varphi(\pm b + \sigma(x \mp b)) & \dots \quad |x| \ge b \end{cases}$$

Finally, let us choose a localization function $j \in C_0^\infty((-a, a))$ and define

$$\Phi_{\sigma,\varepsilon}(x, y) := \varphi_\sigma(x)\,[\chi_1(y) + \varepsilon j(x)^2 \eta_1(y)] \tag{3.2}$$

for any $\sigma,\, \varepsilon > 0$. The main point of the construction is that we modify the factorized function we started with in two mutually disjoint regions, outside and inside the rectangle $J \times (-d_2, d_1)$. Hence the functions φ'_σ and j^2 have disjoint supports. Using this together with the identity

$$\|\varphi'_\sigma\|^2_{L^2(I\!R)} = \sigma \|\varphi'\|^2_{L^2(I\!R)}$$

and the explicit forms of the functions χ_1, η_1, we substitute (3.2) into (3.1) and find after a tedious but straightforward computation

$$\begin{aligned} q[\Phi_{\sigma,\varepsilon}] &= \sigma \|\varphi'\|^2_{L^2(I\!R)} - 4\pi\varepsilon d_1^{-3/2} D^{-1/2} \|j^2\|^2_{L^2(I\!R)} \sin\left(\frac{\pi}{1+\nu}\right) \\ &+ \varepsilon^2 \left\{ \|2jj'\|^2_{L^2(I\!R)} - (\mu_d^2 - \mu_D^2)\, \|j^2\|^2_{L^2(I\!R)} \right\}. \end{aligned} \tag{3.3}$$

By construction, the last two terms on the right side of (3.3) are independent of σ. Moreover, the term linear in ε is negative (recall that $\nu \in (0,1]$), so choosing ε sufficiently small, we can make it dominate over the quadratic one. Finally, we fix this ε and choose a small enough σ to make the right side of (3.3) negative. ∎

Remark: Though it is not the subject of the present paper, we want to note that the same argument demonstrates existence of a bound state in a straight Dirichlet strip with an arbitrarily small protrusion; one has only to replace $J \times [-d_2, 0]$ by a rectangle contained in the protruded part. An alternative proof of this result has been given recently in Ref. 26; these autors also derived an asymptotic formula for the eigenvalue in terms of the protrusion volume.

IV Mode matching

To learn more about the eigenvalues and eigenfunctions in question, we shall now solve the corresponding Schrödinger equation numerically. Since Ω consists of several rectangular regions, the easiest way to do that is by the mode–matching method.

IV.1 The symmetric case

Consider first the situation when $d_1 = d_2 = d$. The Hamiltonian (2.1) then decouples into an orthogonal sum of the even and the odd part, the spectrum of the latter being clearly trivial, *i.e.*, the same as in the case $\ell = 0$. At the same time, the mirror symmetry with respect to the y–axis allows us to consider separately the symmetric and antisymmetric solutions.

We may therefore restrict ourselves to the part of Ω in the first quadrant, with the Neumann boundary condition in the segment $(0, a)$ of the x–axis, and Neumann or Dirichlet condition in the segment $(0, d)$ of the y–axis. We expand the sought solutions in terms of corresponding transverse eigenfunctions

$$\chi_j(y) \;:=\; \sqrt{\frac{2}{d}}\,\sin(\kappa_j y)\,, \quad j=1,2,\dots \tag{4.1}$$

$$\phi_j(y) \;:=\; \sqrt{2}\,\eta_{2j-1}(y) \;=\; \sqrt{\frac{2}{d}}\,\sin(K_{2j-1}(d-y))\,, \quad j=1,2,\dots\,, \tag{4.2}$$

where $\kappa_j := j\kappa_1$ and $K_{2j-1} := (2j-1)K_1$. A natural Ansatz for the solution of an energy $\epsilon\mu_d$, $\frac{1}{4} \le \epsilon < 1$, is

$$\psi(x,y) \;=\; \sum_{j=1}^{\infty} b_j\, e^{q_j(a-x)}\,\chi_j(y) \tag{4.3}$$

for $x \ge a$, where $q_j := \kappa_1\sqrt{j^2-\epsilon}$, and

$$\psi_s(x,y) \;=\; \sum_{j=1}^{\infty} a_j\,\frac{\cosh(p_j x)}{\cosh(p_j a)}\,\phi_j(y)\,, \quad \psi_{as}(x,y) \;=\; \sum_{j=1}^{\infty} a_j\,\frac{\sinh(p_j x)}{\sinh(p_j a)}\,\phi_j(y) \tag{4.4}$$

for $0 \le x \le a$ and the symmetric and antisymmetric cases, respectively, where the longitudinal momentum is defined by $p_j := \kappa_1\sqrt{\left(j-\frac{1}{2}\right)^2-\epsilon}$. It is straightforward to compute the norms of the functions (4.3) and (4.4); since $j^{-1}q_j$ and $j^{-1}p_j$ tend to μ_d as $j\to\infty$, the square integrability of ψ requires the sequences $\{a_j\}$ and $\{b_j\}$ to belong to the space $\ell^2(j^{-1})$.

As an element of the domain of H, the function ψ should be continuous together with its normal derivative at the segment dividing the two regions, $x=a$. Let us first solve this condition formally. The continuity means $\sum_{k=1}^{\infty} a_k\phi_k(y) = \sum_{k=1}^{\infty} b_k\chi_k(y)$; using the orthonormality of $\{\chi_j\}$ we get from here

$$b_j \;=\; \sum_{k=1}^{\infty} a_k(\chi_j,\phi_k)\,. \tag{4.5}$$

In the same way, the normal–derivative continuity at $x=a$ yields

$$q_j b_j \;+\; \sum_{k=1}^{\infty} a_k p_k\tanh(p_k a)\,(\chi_j,\phi_k) \;=\; 0 \tag{4.6}$$

in the Neumann case, and the analogous relation with tanh replaced by coth for Dirichlet. Substituting from (4.5) to (4.6), we can write the equation as

$$Ca \;=\; 0\,, \tag{4.7}$$

where

$$C_{jk} \;:=\; \left(q_j + p_k\left\{\begin{array}{c}\tanh\\ \coth\end{array}\right\}(p_k a)\right)\,(\chi_j,\phi_k) \tag{4.8}$$

in the Neumann and Dirichlet case, respectively, with the two orthonormal bases related by

$$(\chi_j, \phi_k) \,=\, \frac{(-1)^{j-k}}{\pi}\, \frac{2j}{j^2 - \left(k-\frac{1}{2}\right)^2}\,. \tag{4.9}$$

One has to make sure, of course, that the equation (4.8) makes sense, and that one can solve it by a sequence of truncations. It is possible to follow the procedure formulated in Ref. 4. A more direct way, however, is to notice that if ψ is an eigenvector of H, it must belong to the domain of any integer power of this operator. It is easy to check that $\psi \in D(H^n)$ *iff* $\{a_j\}, \{b_j\} \in \ell^2(j^{2n-1})$; hence the sought sequences should belong to $\ell^2(j^s)$ for all $s \ge -1$. This fact also justifies *a posteriori* the interchange of summation and differentiation we have made in the matching procedure.

Consider now the diagonal operator S_r on $\ell^2(j^{-1})$, $(S_r a)_j := j^{-r} a_j$. If C has zero eigenvalue with a fast decaying eigenvector, the same is true for $C^{(s,r)} := S_s C S_r$ with arbitrary non–negative s, r. The last named operator is represented by the matrix

$$C_{jk}^{(s,r)} \,:=\, (q_j + p_k \tanh(p_k a)\,)\, \frac{(-1)^{j-k}}{\pi}\, \frac{2j^{1-s}k^{-r}}{j^2 - \left(k-\frac{1}{2}\right)^2}$$

(for the sake of brevity, we speak about the Neumann case only), so it is Hilbert–Schmidt for r, s large enough, and its eigenvalues can therefore be obtained from a sequence of truncated operators. Since finite matrices pose no convergence problems, the truncation procedure may be applied to the operator C directly.

Of course, $C^{(r,s)}$ may have eigenvectors to which no square–summable eigenvector of C corresponds, because S_r^{-1} is unbounded for $r > 0$. Fortunately, the search for solutions may be terminated once we find the number of them which saturates the upper bound derived in Section 2.

IV.2 An alternative method

A natural modification of the above described procedure is to express $\{a_k\}$ from (4.5) using the orthonormality of $\{\phi_k\}$, and to substitute it into (4.6); then the spectral condition acquires the form

$$b + Kb \,=\, 0\,, \tag{4.10}$$

where

$$K_{jm} \,:=\, \frac{1}{q_j} \sum_{k=1}^{\infty} (\chi_j, \phi_k)\, p_k \tanh(p_k a)\, (\phi_k, \chi_m)\,, \tag{4.11}$$

and the same with $\coth(p_k a)$ in the Dirichlet case.

The two approaches are, of course, equivalent. Solving the equation numerically, however, we truncate not only the matrices but also the series in (4.11). The sequences approximating a given eigenvalue are therefore different. Moreover, in the examples given below we find them monotonous in the opposite sense. The sequences coming from (4.7) were approaching the limiting values from above, while those obtained from (4.10) were increasing; in combination this gives a good idea about the numerical stability of the solution.

IV.3 The asymmetric case

Let us pass now to the case, when the widths of the ducts are nonequal, $d_1 \neq d_2$. Without loss of generality, we may again suppose that $d_2 \leq d_1 = d$. With the mirror symmetry with respect to the y–axis in mind, we shall consider the right–halfplane part of Ω only with the Neumann and Dirichlet condition on the segment $\mathcal{W} := [-d_2, d_1]$ of the y–axis.

To expand the sought solution, we need again suitable transverse bases. In the "connecting part", $0 \leq x \leq a$, we use

$$\eta_k(y) = \sqrt{\frac{2}{D}} \sin(K_k(d_1 - y)), \quad k = 1, 2, \dots, \tag{4.12}$$

where $K_k := kK_1 = k\kappa_1(1+\nu)^{-1}$. On the other hand, for the ducts we choose

$$\chi_j^{(+)}(y) := \sqrt{\frac{2}{d_1}} \sin(\kappa_j y)\, i_+(y), \quad j = 1, 2, \dots, \tag{4.13}$$

$$\chi_j^{(-)}(y) := -\sqrt{\frac{2}{d_2}} \sin(\kappa_j \nu^{-1} y)\, i_-(y), \quad j = 1, 2, \dots, \tag{4.14}$$

where $\kappa_j := j\kappa_1$ and $i_\pm$ are the indicator functions of the intervals $\mathcal{D}_+ := [0, d_1]$ and $\mathcal{D}_- := [-d_2, 0]$, respectively.

The union of the two bases is, of course, an orthonormal basis in $L^2(\mathcal{W})$. Since the numerical computation involves a truncation procedure, we need to introduce a proper ordering. For that we arrange the eigenvalues corresponding to (4.13) to a single nondecreasing sequence. Equivalently, we arrange the numbers j, $k\nu^{-1}$ with $j, k = 1, 2, \dots$ into a nondecreasing sequence (if ν is rational and there is a coincidence, any order can be chosen in the pair); we denote its elements by θ_m,

$$\theta_1 := 1, \quad \theta_2 := \min\{2, \nu^{-1}\}, \quad \text{etc.}$$

The corresponding ordered basis in $L^2(\mathcal{W})$ is

$$\xi_m : \xi_m(y) = \begin{cases} \chi_j^{(+)}(y) & \dots \quad \theta_m = j \\ \chi_j^{(-)}(y) & \dots \quad \theta_m = j\nu^{-1} \end{cases} \tag{4.15}$$

Consider first the even solutions, *i.e.*, the Neumann condition at $x = 0$. A natural Ansatz for a solution of an energy $\epsilon\mu_d$, $(1+\nu)^{-2} \leq \epsilon < 1$, is

$$\psi(x, y) := \sum_{k=1}^{\infty} a_k \frac{\cosh(p_k x)}{\cosh(p_k a)}\, \eta_k(y) \qquad \dots \quad 0 \leq x \leq a,$$

$$\psi(x,y) \;:=\; \sum_{j=1}^{\infty} b_j^{(\pm)}\, e^{q_j^{(\pm)}(a-x)}\, \chi_j^{(\pm)}(y) \qquad \ldots \qquad x \ge a\,;\; y \in \mathcal{D}_\pm\,, \tag{4.16}$$

where

$$p_j \;:=\; \kappa_1 \sqrt{\left(\frac{j}{1+\nu}\right)^2 - \epsilon}\,,$$

and

$$q_j^{(+)} \;:=\; \kappa_1 \sqrt{j^2-\epsilon}\,, \quad q_j^{(-)} \;:=\; \kappa_1 \sqrt{\left(\frac{j}{\nu}\right)^2 - \epsilon}\,.$$

The duct part of (4.16) can be also written in a unified way as

$$\psi(x,y) \;=\; \sum_{m=1}^{\infty} c_m\, e^{r_m(a-x)}\, \xi_m(y)\,, \tag{4.17}$$

where

$$c_m \;:=\; \begin{cases} b_j^{(+)} & \ldots \quad \theta_m = j \\ b_j^{(-)} & \ldots \quad \theta_m = j\nu^{-1} \end{cases} \qquad \text{and} \qquad r_m \;:=\; \begin{cases} q_j^{(+)} & \ldots \quad \theta_m = j \\ q_j^{(-)} & \ldots \quad \theta_m = j\nu^{-1} \end{cases}$$

Using the continuity of the function and its normal derivative at $x = a$ together with the orthonormality of $\{\chi_j^{(\pm)}\}$, we find conditions for the coefficient sequences,

$$b_j^{(\pm)} \;=\; \sum_{k=1}^{\infty} a_k\, (\chi_j^{(\pm)}, \eta_k)\,, \tag{4.18}$$

$$q_j^{(\pm)} b_j^{(\pm)} \;+\; \sum_{k=1}^{\infty} a_k\, p_k\, \tanh(p_k a)\, (\chi_j^{(\pm)}, \eta_k) \;=\; 0\,. \tag{4.19}$$

This can be also written as

$$c_m \;=\; \sum_{k=1}^{\infty} a_k\, (\xi_m, \eta_k)\,, \quad r_m c_m \;+\; \sum_{k=1}^{\infty} a_k\, p_k\, \tanh(p_k a)\, (\xi_m, \eta_k) \;=\; 0\,;$$

substituting from the first equation to the second one, we obtain the spectral condition in the form (4.7) with

$$C_{mk} \;:=\; (r_m + p_k \tanh(p_k a))\, (\xi_m, \eta_k)\,, \tag{4.20}$$

where the overlap integrals are given by

$$\begin{aligned} (\chi_j^{(+)}, \eta_k) \;&=\; \frac{2j}{\pi\sqrt{1+\nu}}\, \frac{\sin\left(\frac{\pi k}{1+\nu}\right)}{j^2 - \left(\frac{k}{1+\nu}\right)^2}\,, \\ (\chi_j^{(-)}, \eta_k) \;&=\; \frac{2j}{\pi} \sqrt{\frac{\nu}{1+\nu}}\, \frac{\sin\left(\frac{\pi k}{1+\nu}\right)}{j^2 - \left(\frac{k\nu}{1+\nu}\right)^2}\,. \end{aligned} \tag{4.21}$$

In the odd case, *i.e.*, Dirichlet condition at $x = 0$, we get the same equation with $\tanh$ replaced by $\coth$ in (4.20).

By a straightforward modification of the above argument, one can check that the coefficient sequences have a faster–than–powerlike decay and the spectral condition can be solved by a sequence of truncations. One can also rewrite the condition in the form analogous to (4.10), $c + Kc = 0$, where

$$K_{jm} := \frac{1}{r_j} \sum_{k=1}^{\infty} (\xi_j, \eta_k)\, p_k \tanh(p_k a)\, (\eta_k, \xi_m)\,. \tag{4.22}$$

V Scattering

The analysis is similar to that of the previous section. The incident wave is supposed to be of the form $\chi_j^{(+)}(y)\, e^{-ik_j^{(+)}x}$ in the upper channel, where we have introduced

$$k_j^{(+)} := \kappa_1 \sqrt{k^2 - j^2}\,, \quad k_j^{(-)} := \kappa_1 \sqrt{k^2 - \left(\frac{j}{\nu}\right)^2}\;;$$

we denote by $r_{jj'}^{(\pm)}$, $t_{jj'}^{(\pm)}$, respectively, the corresponding reflection and transmission amplitudes to the j'–th transverse mode in the upper/lower guide. Due to the mirror symmetry, we can again separate the symmetric and antisymmetric situation with respect $x = 0$ and to write

$$r_{jj'}^{(\pm)} = \frac{1}{2}\left(\rho_{jj'}^{(s,\pm)} + \rho_{jj'}^{(a,\pm)}\right), \quad t_{jj'}^{(\pm)} = \frac{1}{2}\left(\rho_{jj'}^{(s,\pm)} - \rho_{jj'}^{(a,\pm)}\right), \tag{5.1}$$

where $\rho_{jj'}^{(\sigma,\pm)}$, $\sigma = s, a$, are the appropriate reflection amplitudes. In the symmetric case we have the following Ansatz for the solution

$$\begin{aligned}
\psi(x,y) &:= \sum_{\ell=1}^{\infty} a_\ell \frac{\cos(p_\ell x)}{\cos(p_\ell a)}\, \eta_\ell(y) && \dots \quad 0 \le x \le a\,, \\
\psi(x,y) &:= \sum_{j'=1}^{\infty} \left(\delta_{jj'}\, e^{-ik_j^{(+)}(x-a)} + \rho_{jj'}^{(+)} e^{ik_{j'}^{(+)}(x-a)} \right) \chi_{j'}^{(+)}(y) && \dots \quad x \ge a\,;\, y \in \mathcal{D}_+\,, \\
\psi(x,y) &:= \sum_{j'=1}^{\infty} \rho_{jj'}^{(-)} e^{ik_{j'}^{(-)}(x-a)}\, \chi_{j'}^{(-)}(y) && \dots \quad x \ge a\,;\; y \in \mathcal{D}_-\,.
\end{aligned} \tag{5.2}$$

The last two relations can be written also as

$$\psi(x,y) = \sum_{m'=1}^{\infty} \left(\delta_{mm'}\, e^{-ik_m(x-a)} + \rho_{mm'} e^{ik_{m'}(x-a)} \right) \xi_{m'}(y)\,,$$

where

$$\rho_{mm'} := \begin{cases} \rho_{jj'}^{(+)} & \dots \quad \theta_m = j\,,\, \theta_{m'} = j' \\ \rho_{jj'}^{(-)} & \dots \quad \theta_m = j\,,\, \theta_{m'} = j'\nu^{-1} \end{cases} \qquad k_m := \begin{cases} k_j^{(+)} & \dots \quad \theta_m = j \\ k_j^{(-)} & \dots \quad \theta_m = j\nu^{-1} \end{cases}$$

Matching the functions (5.2) smoothly at $x = a$ we arrive in the same way as above at the equation

$$\sum_{m'=1}^{\infty} \left(ik_\ell + p_{m'} \tan(p_{m'} a) \right) (\xi_\ell, \eta_{m'})\, a_{m'} \;=\; 2ik_\ell \delta_{m\ell}\,, \tag{5.3}$$

where the index m corresponds to the incident wave and the overlap integrals are given again by (4.21); in the antisymmetric case on has to replace $\tan$ by $-\cot$. The reflection amplitudes are given then by

$$\rho^{(\pm)}_{m\ell} \;=\; -\delta_{m\ell} + \sum_{m'=1}^{\infty} a^{(\pm)}_{m'} (\xi_\ell, \eta_{m'})\;; \tag{5.4}$$

they determine the full S–matrix via (5.1).

VI The results

VI.1 Bound states

The results of the mode–matching computation are illustrated on Figures 2–4. In accordance with the general results of Section 2 the eigenvalues decrease monotonously with the increasing window width and one can sandwich them between the estimates (2.5). The eigenfunctions decay exponentially out of the "interaction" region. The ground state wavefunction is, of course, positive up to a phase factor; the nodal lines of the excited states are parallel to the y–axis. The last feature illustrates once more that apart of the exponential tails in the ducts, the quantum particle "feels" the window part as a closed rectangular resonator.

It is also interesting to estimate the rate at which the eigenvalues emerge from the continuum. The results of the mentioned paper[26] together with the Dirichlet bracketing allow us to find a simple upper bound for the ground–state energy by means of a single strip with a "blister" whose volume is squeezed to zero. Since the asymptotic formula derived in Ref. 26 applies to "gentle" protrusions, it may be employed if the power with which the bump is scaled transversally is larger than the longitudinal one. Hence the gap between the eigenvalue and the continuum for a narrow window is bound from below by $C(\varepsilon)\ell^{4+\varepsilon} + \mathcal{O}(\ell^5)$ for any $\varepsilon > 0$.

This can be compared with the numerical results. Redrawing the first eigenvalue curve of Fig. 2 and analogous results for $\nu \neq 1$ in the logarithmic scale, we find that the asymptotic behavior is powerlike. The convergence of our method for small ℓ is rather slow; nevertheless, using cut–off dimensions of order 10^3 we get for the power values witnessing clearly that the above bound is saturated,

$$\mu_1(\ell) \;=\; \mu_d - c(\nu)\ell^4 + \mathcal{O}(\ell^5)\,. \tag{6.1}$$

The numerically found coefficient $c(\nu)$ is monotonous and reaches its maximum value for $\nu = 1$; this is the expected behavior as can be seen from a simple bracketing argument. Proving the conjecture (6.1) and finding an analytical expression for $c(\nu)$ remains an open problem; the same can be said about the "coupling–constant thresholds", *i.e.*, the way the other eigenvalues emerge from the continuum.

VI.2 Scattering

The passage of the particle through the window region is determined by the transmission and reflection amplitudes (5.1). The physically interesting quantity is the conductivity. If we suppose, for instance, that the particle comes from the upper right guide and leaves through the upper left one, then the conductivity (denoted conventionally as TP and measured in the standard units $2\,e^2/h$) is given by

$$G(k) \,=\, \sum_{j,j'=1}^{[k]} \frac{k_{j'}^{(+)}}{k_j^{(+)}}\, |t_{jj'}^{(+)}(k)|^2\,, \tag{6.2}$$

and similarly for the other combinations; the summation runs over all open channels. The resonance structure is visible on Figure 5.

Another insight can be obtained by investigating the probability flow distribution associated with the generalized eigenvector (5.2) which is defined in the standard way,

$$\vec{j}(\vec{x}) \,:=\, -i\bar{\psi}(\vec{x})\vec{\nabla}\psi(\vec{x})\,. \tag{6.3}$$

The flow patterns change with the momentum of the incident particle. They exhibit conspicuous vortices at the resonance energies which represent the "trapped part" of the wavefunction; this phenomenon is illustrated on Figure 7. It has been argued in the literature that leaky wires similar to those studied here may serve as switching devices[22]. The vortices which emerge in resonance situations lead to the appearance of a magnetic dipole moment, which might be in principle measured experimentally. In this respect situations with a single well developed vortex such as the one illustrated on Figure 6 are particularly promising.

VI.3 Chaos

Discussing a chaotic behavior of a quantum system, it is useful to start with its classical counterpart, and in particular, its phase space. In the present case of an infinite two–strip "billiard" there are no closed classical trajectories with exception of the obvious zero–measure set, hence one has to consider the scattering, *i.e.*, motion of a point particle bouncing its way through the system; the reflection from the walls is supposed be perfectly elastic.

There are two integrals of motion: the longitudinal component of the momentum, $I_1 = p_x$, and the *modulus* of its transverse part, $I_2 = |p_y|$. Hence the phase space trajectory of the system is restricted to a two–dimensional manifold (invariant surface) in the four–dimensional phase space. However, due to the singularity of corresponding classical flow at the edges of the connecting window, the topology of this surface is not equivalent to that of a two–dimensional cylinder, but rather of a pair of mutually crossed cylinders; similar systems are usually dubbed pseudo–integrable[27]. The topological structure of the invariant surface has a consequence for the quantum counterpart: the system cannot be quantized semiclassically.

On the other hand, the quantum system of coupled waveguides has in view of our previous arguments bound states, even many of them *iff* $\ell\sqrt{\nu} \gg d$. Then one can plot the distribution of the eigenvalue spacing as shown on Figure 8 for a particular value of ν; the character of the distribution does not change as the latter is varied. The natural unfolding means in this case to employ the corresponding momentum value $ip_1 = \sqrt{\mu_d\,(\epsilon - (1+\nu)^{-2})}$. The results differ from typical (unfolded) eigenvalue distributions in billiards, both integrable and chaotic, in the first place due to the existence of the sharp localization around a fixed value. The used statistics (several thousand eigenvalues) does not allow us to tell what is the behavior around zero; we see, however, that the decay off the peak is at least exponential. This differs substantially from a typical behavior of chaotic systems, however, one should not be surprised because all the corresponding eigenfunctions are dominated transversally by the lowest mode, so the bound–state family in our "billiard" is effectively one–dimensional.

It is less trivial whether a chaotic behavior may be manifested in the scattering; recall that spatially restricted pseudo–integrable billiards are known to exhibit the so–called wave chaos[24]. To decide whether a quantum scattering system is chaotic or not, one has to study eigenvalue distribution of the corresponding S–matrix, again properly unfolded, which is expected to conform with that of the Dyson circular ensemble of random matrices[28] in the former case. We have performed this task for the system under consideration numerically, analyzing the distribution of the spacing between two neighboring eigenvalues of the S-matrix. The result is plotted on Figure 9; they are compared with the Wigner and the Poissonian distributions peculiar for the chaotic and non–chaotic situation, respectively. It can be seen that the overall shape of this distribution matches the Poissonian distribution for all spacings large enough; on the other hand, the deformation of the distribution near the origin provides a clear sign of non–integrability of the system. The fact that this non–integrability differs from a typical chaotic behavior can be attributed to the fact that the scattered particle passes the window region "only once" without being bounced to and fro as it is the case of finite billiards.

The absence of the fully developed chaos in the coupled waveguides can also be seen when plotting the coefficients a_ℓ which determine the wavefunction in the interaction region by (5.2) as illustrated on Figure 10. Their distribution remains well localized even for higher energies of the incoming particle, its tail being approximately exponential, while in case of an irregular scattering one would expect a slower decay.

VII Time evolution

Up to now we have discussed the coupled waveguide system from the stationary point of view only. Let us look briefly how the window coupling can affect propagation of wavepackets in the ducts. This problem has a natural motivation: it has been suggested recently [22,29,30] that coupled electron waveguides provide an analogue of the optical directional coupler in the sense that they may switch electrons from one quantum wire to another. Moreover, the authors of Ref. 22 conjectured that the electron switching process should be rather fast due to the direct character of the corresponding resonance, since the electron is not trapped in the interaction region during the resonant switching.

The existence of probability–flow vortices discussed above in the interaction region indicates that this might not be the case, *i.e.*, that the electron dwelling time in the junction may not be generally neglected. To get a better insight we have investigated time evolution of wave packets numerically. This can be achieved by approximating the evolution operator by a Trotter–formula product — see Ref. 12, Sec.VIII.8 — with the Dirichlet boundary condition replaced by a very steep and narrow potential barrier localized along the boundary; the latter has been chosen in such a way that the dynamics of the system was equivalent to the dynamics of the true Dirichlet problem for all times taken into account, *i.e.*, that the tunneling leak was negligible during that period.

The kinetic– and potential–part factors of the evolution operator are then multiplication operators in the momentum and coordinate representation, respectively; the passage between the two representations has been realized by means of the two–dimensional Fast Fourier Transform method[31] with a grid of $2^9 \times 2^7$ points. The time evolution of a wavepacket approaching the junction through the upper right arm of the structure is plotted on Figure 11. The incoming wavefunction was chosen as $\psi(x,y) := g(x)\chi_1^{(+)}(y)$, where $g(x) := \exp\{-a(x-x_0)^2 + ikx\}$ with suitably chosen parameters a, x_0 .

The difference between the resonant and nonresonant situation is clearly visible. In the first case the electron stays in the junction region and escapes only slowly, while the electron whose momentum is localized around a slightly different but nonresonant value of momentum passes the junction "ballistically". Wang and Guo[22] based the mentioned conjecture — which in a realistic situation would lead to ultrashort switching times of a few *ps* only — on a concept of transmitivity of coupled waveguides leaning on a classical intuition. As we have said in the introduction and demonstrated in the previous sections, this may be a false guide when quantum systems are considered. The example of time evolution offers another illustration. During the resonance–scattering process the evanescent–mode amplitudes inside the quantum wire are considerably enhanced; as a result the electron is trapped temporarily inside the juction. The probability of finding it there in the resonant and nonresonant case, respectively, is shown on Figure 12. It is desirable to perform the time–delay analysis for the present model, in particular, to confirm that the "switching time" of the coupler is inversely proportional to the resonance width.

Acknowledgement

The work has been partially supported by the Grants AS No.148409 and GA CR No.202–93-1314.

References

[1] R. Hempel, L.A. Seco, B. Simon: "The essential spectrum of Neumann Laplacians on some bounded singular domains", J. Funct. Anal. **102**, 448–483 (1991)

[2] B. Simon: "The Neumann Laplacian of a jellyroll", Proc. Amer. Math. Soc. **114**, 783–785 (1992)

[3] P. Exner, P. Šeba: "Bound states in curved quantum waveguides", J. Math. Phys. **30**, 2574–2580 (1989)

[4] P. Exner, P. Šeba, P. Šťovíček: "On existence of a bound state in an L–shaped waveguide", Czech. J. Phys. **B39**, 1181–1191 (1989)

[5] R.L. Schult, D.G. Ravenhall, H.W. Wyld: "Quantum bound state in classically unbound system of crossed wires", Phys. Rev. **B39**, 5476–5479 (1989)

[6] J. Goldstone, R.L. Jaffe: "Bound states in twisting tubes", Phys. Rev. **B45**, 14100–14107 (1992)

[7] G. Dunne, R.L. Jaffe: "Bound states in twisted Aharonov–Bohm tubes", Ann. Phys. **233**, 180–196 (1993)

[8] P. Duclos, P. Exner: "Curvature–induced bound states in quantum waveguides in two and three dimensions", Rev. Math. Phys. **7**, 73–102 (1995)

[9] P. Exner: "A model of resonance scattering on curved quantum wires", Ann. Physik **47**, 123–138 (1990)

[10] P. Duclos, P. Exner, P. Šťovíček: "Curvature–induced resonances in a two–dimensional Dirichlet tube", Ann. Inst. H. Poincaré **62**, 81–101 (1995)

[11] P. Duclos, P. Exner, B. Meller: "Exponential bounds on curvature–induced resonanaces in a two–dimensional Dirichlet tube", *submitted for publication*

[12] M. Reed, B. Simon: *Methods of Modern Mathematical Physics, I. Functional Analysis, IV.Analysis of Operators*, Academic Press, New York 1972, 1978.

[13] C.M. Savage, S. Markensteiner, P. Zoller: "Atomic waveguides and cavities from hollow optical fibres", in *Fundamentals of Quantum Optics III* (S. Eklotzky, ed.), Springer, Berlin 1993.

[14] P. Exner, P. Šeba: "Trapping modes in a curved electromagnetic waveguide with perfectly conducting walls", Phys. Lett. **A144**, 347–350 (1990)

[15] J.P. Carini, J.T. Londergan, K. Mullen, D.P. Murdock: "Bound states and resonances in quantum wires", Phys. Rev. **B46**, 15538–15541 (1992)

[16] J.P. Carini, J.T. Londergan, K. Mullen, D.P. Murdock: "Multiple bound states in sharply bent waveguides", Phys. Rev. **B48**, 4503–4514 (1993)

[17] B. Simon: "The bound state of weakly coupled Schrödinger operators in one and two dimensions", Ann. Phys. **97**, 279–288 (1976)

[18] R. Blanckenbecler, M.L. Goldberger, B. Simon: "The bound states of weakly coupled long-range one-dimensional quantum Hamiltonians", Ann. Phys. **108**, 69–78 (1977)
[19] Y. Hirayama, Y. Tokura, A.D. Wieck, S. Koch, R.J. Haug, K. von Klitzing, K. Ploog: "Transport characteristics of a window–coupled in–plane–gated wire system", Phys. Rev. **B48**, 7991-7998 (1993)
[20] Ch. Kunze: "Leaky and mutually coupled quantum wires", Phys. Rev. **B48**, 14338–14346 (1993)
[21] I.A. Larkin, E.V. Sukhorukov: "Method to investigate the random potential in a quantum point contact", Phys. Rev. **B49**, 5498–5507 (1994)
[22] Jian Wang, Hong Guo: "Time–dependent transport in two–dimensional quantum–wire structures", Phys. Rev. **B48**, 12072–12075 (1993)
[23] P. Exner, M. Tater: "A one–band model for a weakly coupled quantum–wire resonator", Phys. Rev. **B50**, 18350–18354 (1994)
[24] A. Shudo, Y. Shimizu, P. Šeba, J. Stein, H.J. Stockmann, K. Życzkowski: "Statistical properties of spectra of pseudointegrable systems", Phys. Rev. **E49**, 3748–3756 (1994)
[25] K. Życzkowski: "Classical and quantum billiards", Acta Phys. Polonica **23**, 245–270 (1992)
[26] W. Bulla, F. Gesztesy, W. Renger, B. Simon: "Weakly coupled bound states in quantum waveguides", *submitted for publication*
[27] P.J. Richens, M.V. Berry: "Pseudointegrable systems in classical and quantum mechanics", Physica **D2**, 495–512 (1981)
[28] R. Blumel, U. Smilansky: "Classical irregular scattering and its quantum mechanical implications", Phys. Rev. Lett. **60**, 477–480 (1988)
[29] J.A. del Alamo, C.C. Eugster: "Quantum field–effect directional coupler", Appl. Phys. Lett. **56**, 78–80 (1990)
[30] N. Tsukada, A.D. Wieck, K. Ploog: "Proposal of novel electron wave coupler devices", Appl. Phys. Lett. **56**, 2527–2529 (1990)
[31] D. Kosloff, R. Kosloff: "Absorbing boundaries for wave propagation problems", J. Comput. Phys. **63**, 363–376 (1986)

Figure captions

Figure 1 Laterally coupled quantum waveguides

Figure 2 Bound–state energies *vs.* the window width ℓ in the symmetric case.

Figure 3 The ground–state eigenfunction in the symmetric case for $\ell/d = 0.3$.

Figure 4 The eigenfunction of the second excited state in the unsymmetric case, $\nu = 1/2$, for $\ell/d_1 = 1.08$.

Figure 5 The conductivity for the particle coming from the right in the upper duct as a function of the momentum k and the width d_2 of the lower tube for $d_1 = \pi,\ \ell = 2$. (a) The particle leaves through the upper left channel. A deep resonance is clearly visible. (b) The particle leaves through the lower left channel. The conductivity is zero when there are no propagating modes in the lower part.

Figure 6 The quantum probability flow (6.3) for the symmetric situation, $\nu = 1$, in the resonance and non–resonance situation, respectively. The appearance of vortices associated with the resonance scattering is obvious.

Figure 7 A single vortex corresponding to the sharp stopping resonance of Figure 6a. The conductivity is small in this situation so the waveguide system is closed for the electron transport.

Figure 8 The unfolded level–spacing distibution of the symmetric and antisymmetric bound states for $\nu = 2(1+\sqrt{5})^{-1}$.

Figure 9 The unfolded level–spacing distribution for the S–matrix corresponding to $\nu = 2/\pi$ and averaged over momentum, in comparison with the Poisson and Wigner distribution.

Figure 10 The absolute value of the coefficients a_ℓ of eq.(5.2) in the symmetric case for $\nu = 2/\pi$ and $k = 28.432$; the particle is supposed to be initially in the 18-th transverse mode.

Figure 11 The time evolution of the wavepacket inside the junction with $\nu = 2/\pi$ plotted for times $t = 0$, 5, 10, 15, and 20, respectively. (a) The resonance case with $k = 1.4242$, (b) the near–to–resonance situation, $k = 1.48$.

Figure 12 The probability that the electron will be found within the junction as a function of time evaluated for the same parameters as on Figure 11.